

# An overview of the effect of various interlayer materials and boundary conditions on delaminated glass plates

Ebru Dural<sup>1,2</sup> 

<sup>1</sup> Department of Civil Engineering, Adnan Menderes University, 09100 Aydin, Turkey

<sup>2</sup> Department of Technical Programs, Kyrgyz-Turkish Manas University, 720044 Bishkek, Kyrgyz Republic  
E-mail: ebru.dural@adu.edu.tr

## ABSTRACT

This study presents a large-deflection mathematical analysis of a laminated glass plate that has suffered initial delamination. Three distinct interlayer types are taken into consideration in order to examine how the type of interlayer affects the behavior of delaminated glass plates. The plate is subjected to uniform pressure. The analysis is based on solving five nonlinear partial differential equations relating the lateral deflections and stresses to the applied load. The established solution approach is presented in a simple form suitable for analyzing various loads, geometries, material properties and boundary conditions. Two boundary conditions – fixed and simply supported edges – are taken into consideration for plates. It is established that interlayer type has a major effect in determining the delamination strength of laminated glass. Design engineers can use the current research findings to build laminated glass for structural applications.

**Keywords:** laminated glass, delamination, plate, interlayer.

## INTRODUCTION

Glass and laminated glass have become indispensable materials for the construction industry due to their versatility, aesthetic appearance and structural performance, and even waste glass is now being used in the construction industry (54, 55). Laminated glass is a type of safety and security glass which is created by heating and pressing two or more glass panels with a unique binding agent called polyvinyl butyral (PVB) interlayer. Even in the event of a break, the interlayer helps to maintain and support the glass to produce a strong, homogeneous layer. There are many different interlayer used in the glazing industry to produce laminated glass. Mechanical performance, blast performance, durability, availability, material cost, manufacturing cost, and optical clarity are factors to consider when selecting a good interlayer. Several types of interlayer materials are commercially available; however, the most commonly used are polyvinyl butyral (PVB), ethylene vinyl acetate (EVA), sentryglas plus (SGP), polyurethane (TPU) and cast resin (CIP).

Because of its flexibility, cost-effectiveness, good adherence and optical clarity, PVB is the primary interlayer in the glazing industry. On the other hand, EVA has high resistance against moisture and can be used under high moisture levels. Since SGP is more rigid and stiffer than other interlayers, it provides greater strength and less deflection. Despite the high strength and rigidity it provides, SGP costs a lot more than PVB and due to this feature, its use in the glass industry is limited.

After being invented, laminated glass was the focus of the automotive industry, and there were few technical patent filings concerning its application. In the 1970s, research on the structural application of laminated glass started to gain attention [1]. Researchers studied the structural behavior of laminated glass through theoretical and experimental means [2–8] in the 1980s. Research on the real behavior of laminated glass was significantly enhanced in the 2000s by theoretical [9–15] numerical [16–20] and experimental [21–24] studies. Studies revealed that layered and monolithic situations are the two limiting scenarios for laminated glass's structural behavior [20, 32].

In light of previously conducted research, it has been observed that the structural performance of laminated glass is significantly influenced by delamination under various loading conditions, including static [25], dynamic [26], impact [27, 28] and blast [29, 30] loadings.

The process by which the interlayer of the composite separates from the glass surface is known as delamination. Although laminated glass has been used in buildings for a long time the possibility of delamination is a major concern about its safety. Water immersion is the main cause of delamination, and as the area impacted by immersion is typically near the bottom of the glass, delamination typically occurs from the bottom up. Because of this, the foggy, opaque appearance, which is one of the earliest obvious symptoms of glass delamination, gradually rises to the top of the glass and naturally, the discoloration may appear unsightly. Even if the cause of the delamination is resolved, the delamination process quickly intensifies once it begins, necessitating the replacement of the glass. Although delamination cannot be completely removed, it can be slowed down or even stopped from spreading with the right corrective procedures. Also, when chosen appropriately, these measures can cover up the delamination by improving the look. Initial delamination is result of pure manufacturing process. The unsmooth structure of tempered glass which cause surface stress, local bowing, and edge warping; dirty glass surface; Unsuitable site of application in terms of temperature and humidity; Use of incompatible sealants with the interlayer in lamination are the possible reasons of initial delamination.

Since the mechanical properties of interlayer materials greatly affect the structural integrity of laminated glass, the effect of different interlayers on delaminated samples will also be different. Although delamination affects laminated glass units as much as other composite materials, there haven't been many studies done on the structural characterization of delaminated glass [33–42]. From this angle, the ability to forecast how laminated glass will behave when it is subjected to delamination is essential for creating engineering applications. Examining adhesion and delamination between the interlayer and glass was the goal of some research and numerical cohesive zone models were used to simulate delamination and modify adhesion parameters [43–46]. The delamination analysis of laminated glass has been the subject of numerous numerical investigations because of their

convenience in solving difficult problems [33, 36]. Additionally, experimental research on the problem of laminated glass delamination was conducted [47–51]. A variety of testing methods exist to evaluate or quantify the Laminated glass interfacial adhesion, such as peel tests, pull-off tests, pummel tests, compression shear tests, and the through-cracked tensile/bending tests.

Using experimental tensile tests on samples of shattered laminated glass, Hooper et al. [33] investigated the delamination characteristics of laminated glass windows under blast stress. They noticed that a considerable quantity of energy is absorbed during the delamination process.

The application of laminated glass units has risen significantly in the past few decades in a variety of industrial sectors, including the marine, automotive, aerospace, and civil engineering sectors. Analyzing laminated glass's mechanical behavior has become more and more necessary as a result. The mechanical behavior of laminated units is the primary focus of the studies now conducted on laminated glass; delamination-related research is rarely highlighted. Furthermore, the amount of research that examines the effect of interlayers on the nonlinear behavior of delaminated glass units is much smaller than the scope of engineering applications for this material.

The goal of the current study is to examine how interlayer type affects delamination, one of the most frequent issues with using laminated glass. To evaluate the effect of three different types of interlayers on the delamination strength of laminated glass plates the mathematical model developed by Dural [31] is applied. The boundary conditions are important to the model, and different boundary conditions will lead to different effects on the strength of the laminated glass plate. Finally, the delamination and boundary conditions relationships of the plate are discussed. To assess how the boundary conditions affect, the results obtained by using the fixed boundary conditions are compared with those obtained by using the simple supported ones.

## RESULTS OF MATHEMATICAL MODEL

In the laminated glass unit, the interlayer that permits the glass to be bonded together is inserted between two glass panes, and the assembly is then placed in an autoclave under high pressure and temperature, causing the interlayer to adhere

to the glass. Mechanically, single and multiple-layered glass plates require distinct treatment. The elastic behavior of monolithic glass is a well-defined, fundamental structural mechanic problem but laminated constructions differ; determining the increased load-bearing capacity induced by interlayer contact remains a difficulty due to two reasons mentioned below:

First of all, the properties of the glass and the material interlayer are entirely different. At room temperature, the corresponding modulus of the interlayer ranges from 1 to 400 MPa, whereas the shear modulus of the glass is approximately 28 GPa. Highly viscoelastic material PVB has a large temperature dependency for this reason at higher temperature; the shear modulus is predicted to drop even further. Secondly, even when carrying their weight, they undergo significantly large lateral displacements affecting the structure’s reaction and resulting in geometric nonlinearity.

For the reasons stated above, the classical assumption that the plane section of a system before deformation stays plane after distortion is unrealistic for laminated glass units. A more accurate and comprehensive model for analyzing laminated glass structures is required. Aşık [32] developed a nonlinear mathematical model for analyzing laminated glass plates, which Dural [31] amended in 2023 to account for initial delamination. Aşık’s five nonlinear partial differential equations were modified for delaminated regions of the plate by Dural. [31] The present research focuses on the mechanical performance of structural glass with initial delamination and laminated with ethylene vinyl Acetate (EVA), Sentryglas plus (SGP), and polyvinyl butyral (PVB) interlayers. Dural’s [31] model is used to assess the effect of interlayers on the mechanical behavior of delaminated glass units subjected to different boundary conditions. In the derivation, the variational principle was used to generate equations for lateral and in plane displacements, which were then numerically solved using an iterative technique. The solution technique yielded lateral and in-plane displacements as well as stresses. The model was developed based on the premise that the interlayer primarily transmits shear forces while experiencing minimal compression in the lateral direction. This model was validated using the results of performed experiments and created finite element model [52]. The present research focuses on the mechanical performance of structural glass with initial delamination and laminated with ethylene

vinyl Acetate (EVA), Sentryglas plus (SGP), and polyvinyl butyral (PVB) interlayers.

The laminated glass plate utilized in this analysis has dimensions of 1 × 1 meter. It is composed of two glass layers of thickness 5 mm and an interlayer of thickness 0.76 mm. The modulus of elasticity of glass is 70 GPa and the Poisson’s ratio is 0.22. Three laminated glass panels with various interlayer materials (PVB, EVA, and SGP) positioned between two glass layers were examined in this study. The current study considers three distinct interlayers: Ethyl Vinyl Acetate, Polyvinyl Butyral, and Sentryglas Plus. Shear modulus of interlayers are given in Table 1. A 20 × 20 finite difference mesh is selected to analyze the problem and it is subjected to a static lateral pressure that increases consistently until it reaches a maximum pressure near 10 kPa. Detailed explanation about the derivation of governing equations, solution process and validation of the model are given by Dural [31]. Since finite difference method requires less computational power and time and gives good results for regular geometries it is preferred as a suitable tool for the solution.

### Results of a fixed supported laminated glass plate with initial delamination

To benefit from symmetry, the study examines one-fourth glass plate. Figure 1 illustrates how axes are taken. Considering a and b to represent half the length of the plate side, the boundary conditions for a unit that is fixed supported under uniform pressure are outlined as follows:

- At  $x = 0$ ;  $u_1 = 0$ ;  $e_{1xy} = 0$ ;  $u_2 = 0$ ;  $e_{2xy} = 0$ ;  $w_x = 0$
- At  $x = a$ ;  $e_{1x} + v_{e1y} = 0$ ;  $e_{1xy} = 0$ ;  $e_{2x} + v_{e2y} = 0$ ;  $e_{2xy} = 0$ ;  $w = 0$ ;  $w_x = 0$ ;
- At  $y = 0$ ;  $v_1 = 0$ ;  $e_{1xy} = 0$ ;  $v_2 = 0$ ;  $e_{2xy} = 0$ ;  $w_y = 0$ ;
- At  $y = b$ ;  $e_{1x} + v_{e1y} = 0$ ;  $e_{1xy} = 0$ ;  $e_{2x} + v_{e2y} = 0$ ;  $e_{2xy} = 0$ ;  $w = 0$ ;  $w_y = 0$

In the above equations,  $u_1$  and  $u_2$  are the in-plane displacement of the upper and lower glasses

**Table 1.** Shear modulus of interlayer materials

Interlayer material	Shear modulus (kPa)
Ethyl vinyl acetate	5300
Polyvinyl butyral	1287
Sentryglas plus	111000

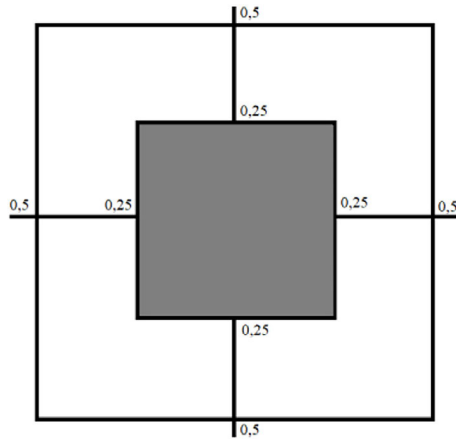


Figure 1. Location of delamination

in the x direction,  $v_1$  and  $v_2$  are the in-plane displacements in the y direction for the upper and lower glasses and  $w$  is the lateral displacement.  $e_{1x}$ ,  $e_{1y}$  and  $e_{1xy}$  are the strains of the upper layer while  $e_{2x}$ ,  $e_{2y}$  and  $e_{2xy}$  are the strains of the lower glass layer. Figure 1 depicts delaminated portion of the glass plate. It is assumed that there

is no bond between the layers in the delaminated zone, which is situated in the center of the unit as can be seen.

Figure 2 shows the load-lateral deflection curves of laminated and delaminated glass plates with various interlayers. As can be seen in the above figure, the delaminated region is at the center of the unit and accounts for 25% of the glass area. Plates exhibit nonlinear behavior due to the membrane forces developing under fixed-end conditions. The deflection of delaminated and laminated glass units connected by PVB interlayer (PVB-connected units) is greater than those of delaminated and laminated glass units connected by EVA interlayer (EVA-connected units) and delaminated and laminated glass units connected by SGP interlayer (SGP-connected units). As detailed in the figure, deflection of undelaminated glass units is small compared with the deflection of delaminated glass units and the effect of delamination is more visible for SGP-connected units. The graph in Figure 3 is

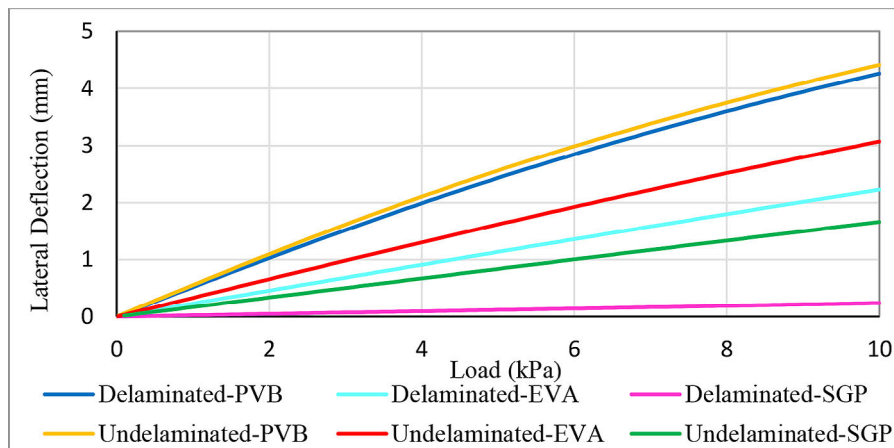


Figure 2. Pressure versus maximum deflection

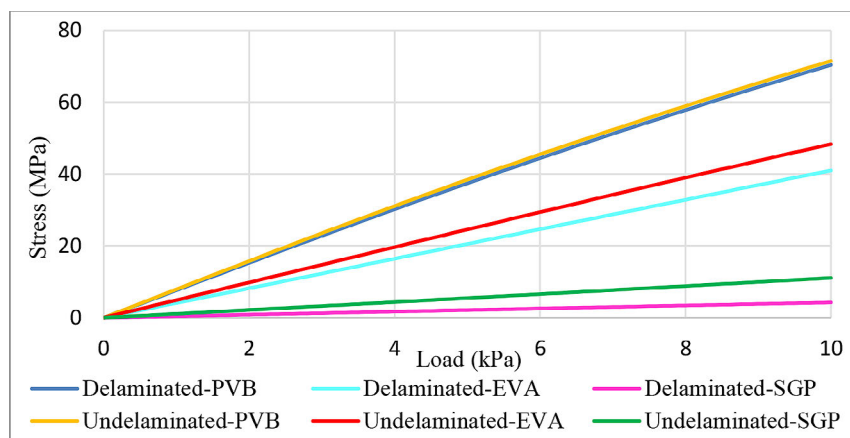


Figure 3. Pressure versus maximum stress

designed to illustrate the comparisons between the maximum stress values. Stresses of SGP-connected units are nearly 7 times smaller than those of PVB-connected units.

Lateral deflections along the diagonal of the quarter plate units are given in Figure 4. Their values peak at the center and diminish to zero at the edge of the plate. Deflection lines display a double curvature as a result of nonlinearity. While the difference between deflections is greatest for SGP-connected units, it is lowest for PVB-connected ones.

Figure 5 shows the variation of maximum principal stress along the diagonal of the quarter plate. It is observed that the maximum principal stresses are tension along the diagonal on the upper plate, and tension and compression on the lower surface.

Maximum principal stress distributions over the upper and lower surfaces of the cross-section are plotted in Figures 6–11 for the three types of interlayer with and without delamination. With SGP and EVA-connected plates, the effects of delamination are more easily visible in the stress

distribution. Both tension and compression zones are observed through the cross section. While the upper surface principal stresses are compressive at the center, they are tension at the unit's edge. The distribution of stresses on the lower surface exhibits a reverse pattern. The stress distributions of the delaminated and undelaminated glass plates attached to the PVB exhibit similarities, as illustrated in Figures 10 and 11. Additionally, it is observed that undelaminated units show somewhat larger strains in comparison to delaminated ones. On the other hand, the lower surface stress distributions change when delamination is present. In the case of delaminated plate, lower surface stresses are maximum at the boundary of the delaminated zone, while they are maximum at the center of the undelaminated plate. The variations in shear modulus between the interlayers can be the cause of their dissimilar behaviors. Additionally, a zero stress area is shown on the upper and lower surfaces of the plate. The specified area is near the plate's corner on the lower surface, whereas it is near the center on the upper surface.

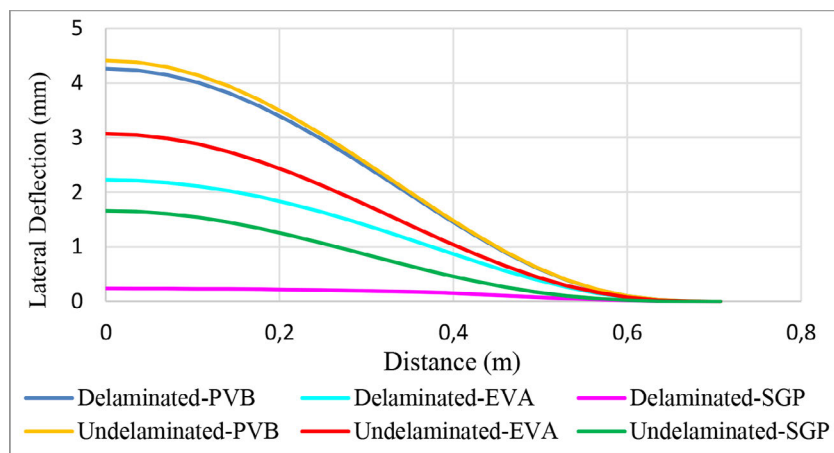


Figure 4. Lateral displacement variation along the diagonal of fixed supported plate

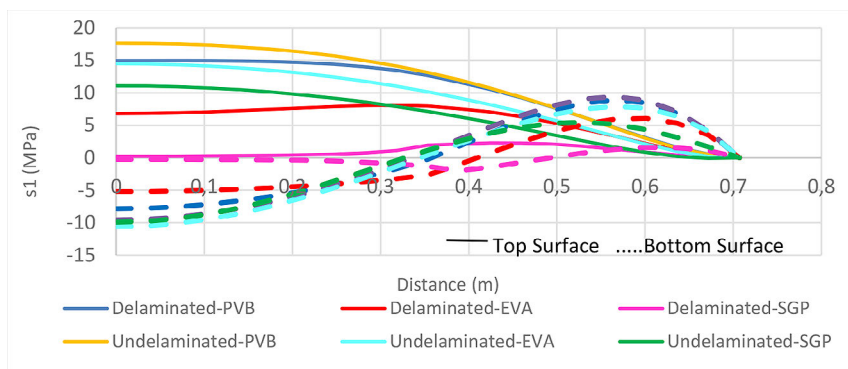


Figure 5. Variation of the maximum principal stress over the fixed supported plate's diagonal

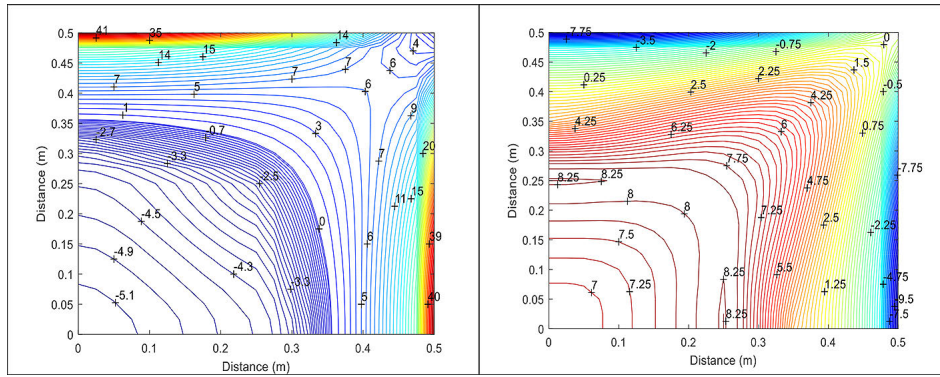


Figure 6. Maximum principal stress contours of EVA-connected delaminated unit for 10 kPa pressure a) upper surface b) lower surface

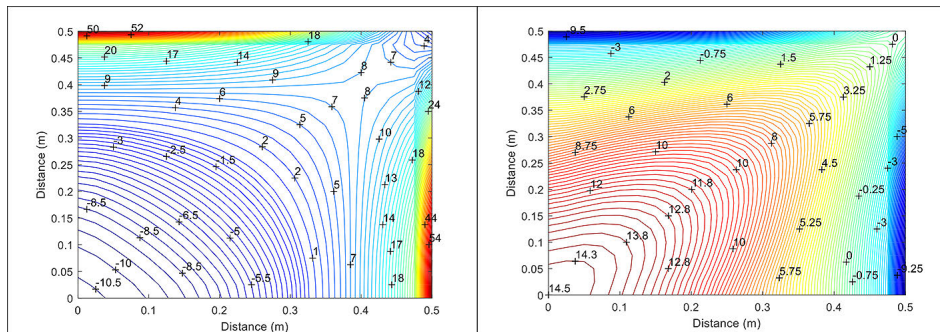


Figure 7. Maximum principal stress contours of EVA-connected undelaminated unit for 10 kPa pressure a) upper surface b) lower surface

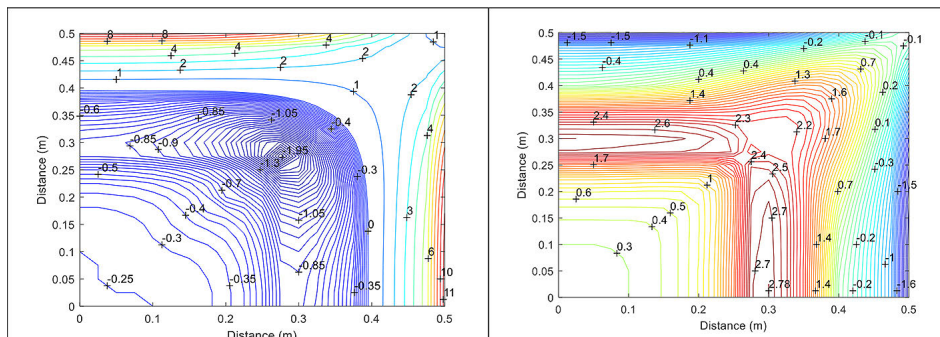


Figure 8. Maximum principal stress contours of SGP-connected delaminated unit for 10 kPa pressure a) upper surface b) lower surface

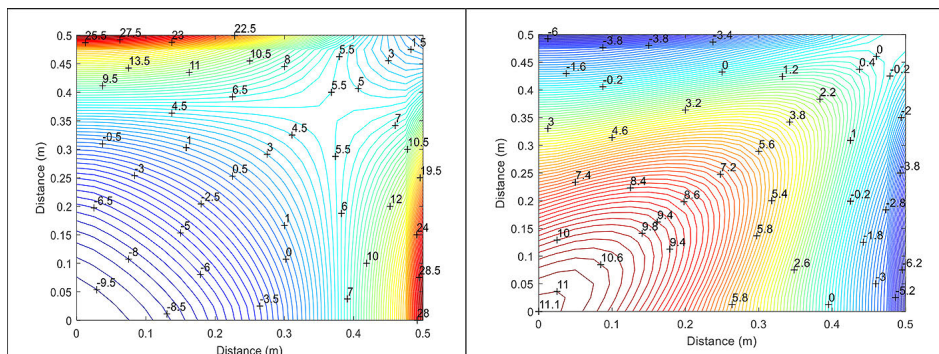
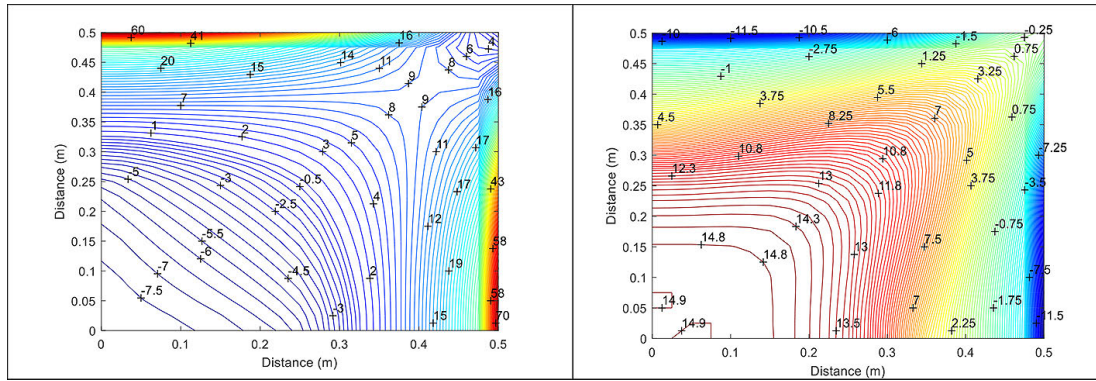
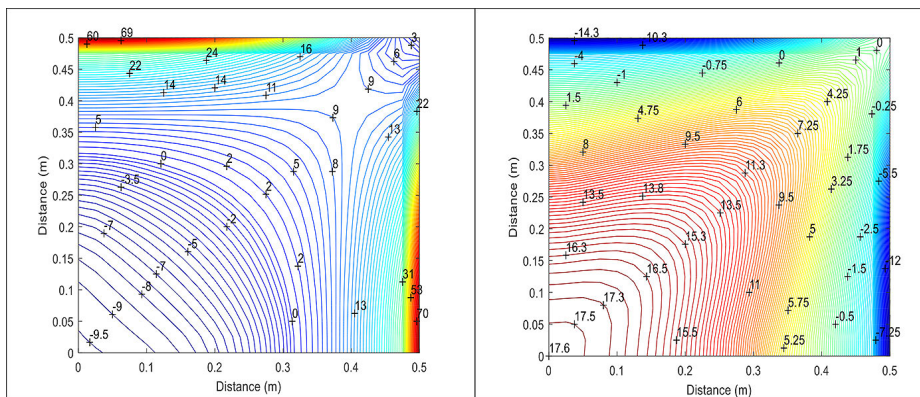


Figure 9. Maximum principal stress contours of SGP-connected undelaminated unit for 10 kPa pressure a) upper surface b) lower surface



**Figure 10.** Maximum principal stress contours of PVB-connected delaminated unit for 10 kPa pressure  
a) upper surface b) lower surface



**Figure 11.** Maximum principal stress contours of PVB-connected undelaminated unit for 10 kPa pressure  
a) upper surface b) lower surface

### Results of a simply supported laminated glass plate with initial delamination

To assess how boundary conditions affect the functionality of laminated glass plate subjected to delamination, a simply supported unit is also examined. The boundary conditions for simply supported units are outlined below:

- At  $x = 0$ ;  $u_1 = 0$ ;  $e_{1xy} = 0$ ;  $u_2 = 0$ ;  $e_{2xy} = 0$ ;  $w_x = 0$
- At  $x = a$ ;  $e_{1x} + v_{e1y} = 0$ ;  $e_{1xy} = 0$ ;  $e_{2x} + v_{e2y} = 0$ ;  $e_{2xy} = 0$ ;  $w = 0$ ;  $w_{xx} = 0$
- At  $y = 0$ ;  $v_1 = 0$ ;  $e_{1xy} = 0$ ;  $v_2 = 0$ ;  $e_{2xy} = 0$ ;  $w_y = 0$
- At  $y = b$ ;  $e_{1x} + v_{e1y} = 0$ ;  $e_{1xy} = 0$ ;  $e_{2x} + v_{e2y} = 0$ ;  $e_{2xy} = 0$ ;  $w = 0$ ;  $w_{yy} = 0$

Figure 12 represents the load versus lateral deflection of the simply supported plate and the deflection of the simply supported unit approximately double that of the fixed supported unit. Compared to the fixed supported plate, the effect of delamination is observed to be more

noteworthy for the simply supported unit. Stress versus load distribution is given in Figure 13 and simply supported plates have stresses that are almost half of those of fixed supported plates.

Delamination significantly influences the performance of laminated glass panels connected by SGP interlayer. Concerning fixed supported units, there are more observable differences in the behaviors of simply supported PVB-connected units. Lateral deflections along the diagonal of the plate are given in Figure 14.

Figures 15 illustrates the maximum principal stresses along the diagonal of both the upper and lower surfaces of the plate. It should be emphasized that, in Figure 15, absolute principal stresses take place at the lower plate as tension. The maximum principal stress on the lower plate is tension, but the upper plate has both tension and compression. For undelaminated units, the maximum principal stresses are located in the middle of the plate. For delaminated units, the maximum stress site varies along the diagonal line. For the

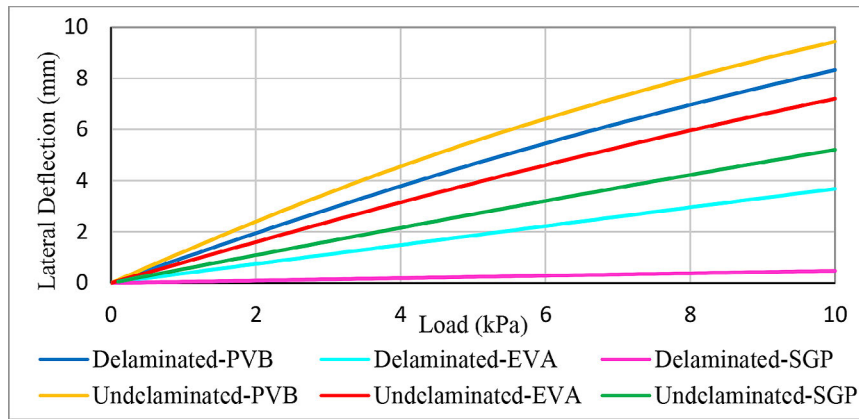


Figure 12. Pressure versus maximum deflection

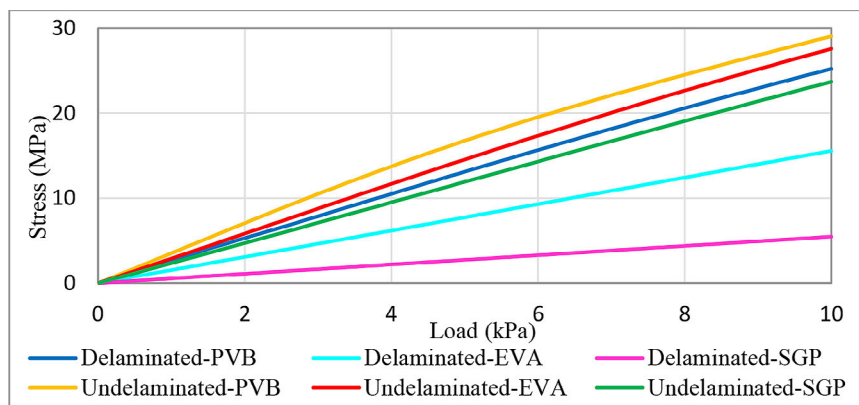


Figure 13. Pressure versus maximum stress

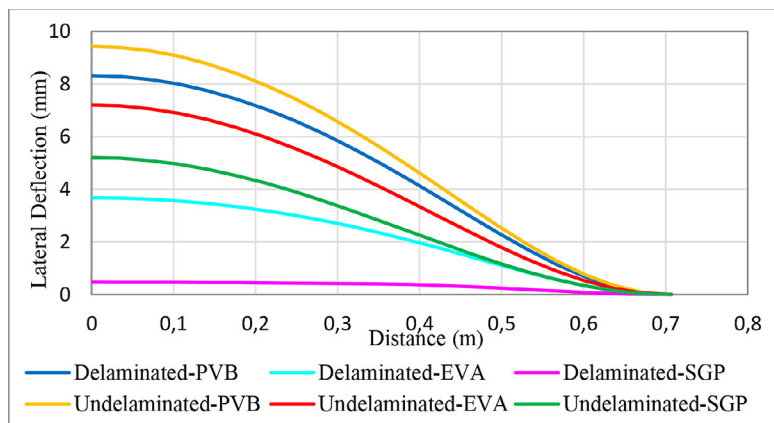


Figure 14. Variation of lateral displacement along the simply supported plate's diagonal

PVB connected delaminated unit it is close to the midpoint of the diagonal and it is closest to the corner for SGP connected unit. At a point along the diagonal line between 0.4 and 0.5 meters from the unit's center, the maximum principal stresses on the upper plate are zero.

Figures 16 and 17 show stress patterns on the upper and lower surfaces of a PVB-connected

plate under 10 kPa applied pressure. Tension and compression stresses are present on the upper surface of the delaminated and undelaminated units connected by PVB, while tension stresses are present on the lower surface. Figures show that delamination alters both the position of maximum stress and the stress distributions. Undelaminated unit stresses are higher than those of the



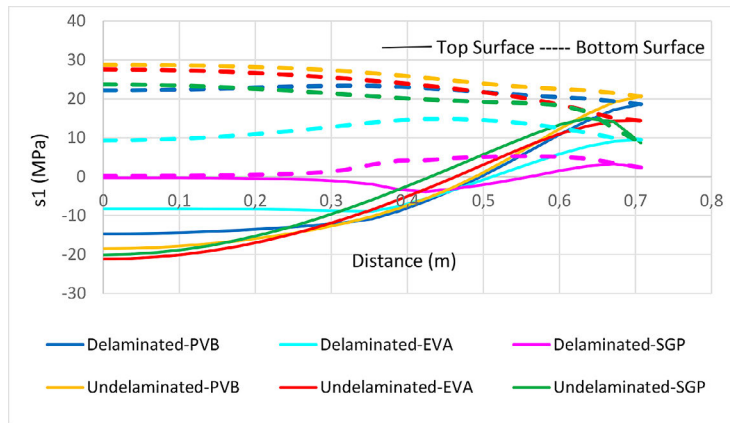


Figure 15. Variation of the maximum principal stress over the simply supported plate’s diagonal

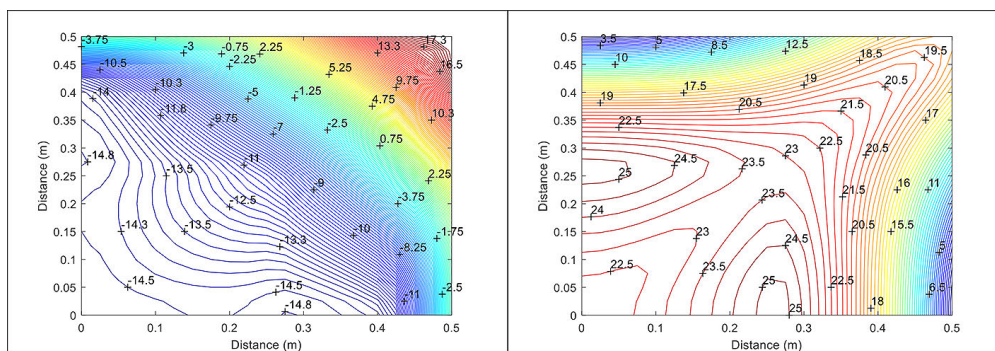


Figure 16. Maximum principal stress contours of PVB-connected delaminated unit for 10 kPa pressure  
a) upper surface b) lower surface

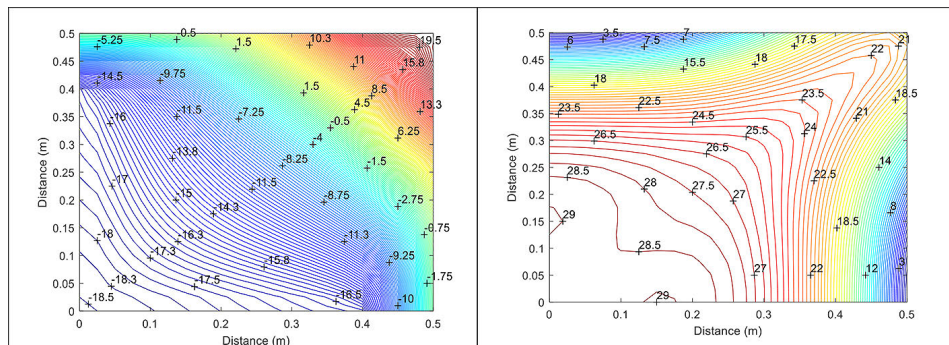


Figure 17. Maximum principal stress contours of PVB-connected undelaminated unit for 10 kPa pressure  
a) upper surface b) lower surface

delaminated unit. On both surfaces, the maximum stress position is moving via the delaminated region’s border.

Observe how the contours alter in shape as the aspect ratio fluctuates. As the aspect ratio increases, areas of significant deflection and stress are not confined to the center of the plate, and the performance begins to resemble that of one-way plates.

Stress contours of laminated glass units connected by EVA are given in Figures 18 and 19.

It seems that although tensile stress appears on the lower surface, both compressive and tensile stresses appear to develop on the upper surfaces. On the lower surface, location of maximum stress is at the center of the plate and it moves along the diagonal towards the corner of the unit. The upper surface maximum principal stress is at the edge of the delaminated plate as tension while it is compression and at the center for undelaminated plate.

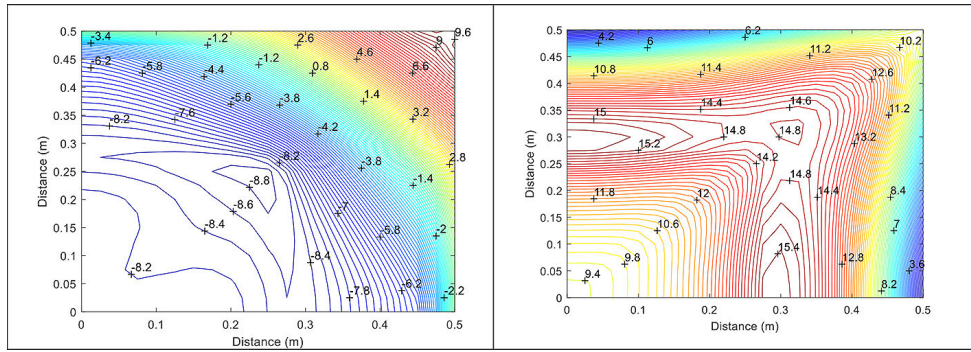


Figure 18. Maximum principal stress contours of EVA-connected delaminated unit for 10 kPa pressure  
a) upper surface b) lower surface

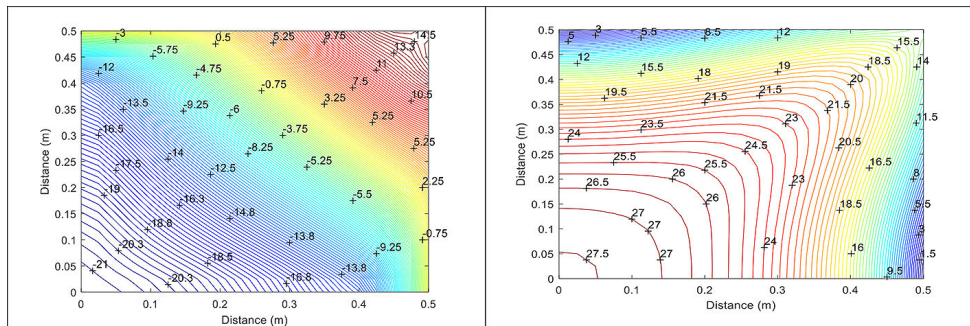


Figure 19. Maximum principal stress contours of EVA-connected undelaminated unit for 10 kPa pressure  
a) upper surface b) lower surface

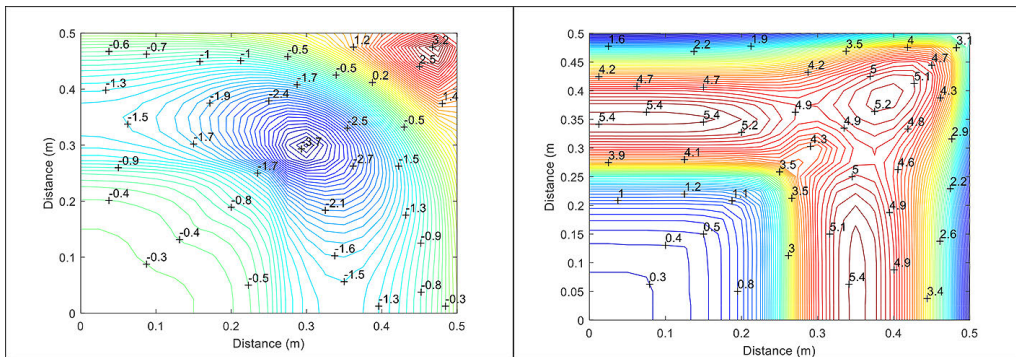


Figure 20. Maximum principal stress contours of SGP-connected delaminated unit for 10 kPa pressure  
a) upper surface b) lower surface

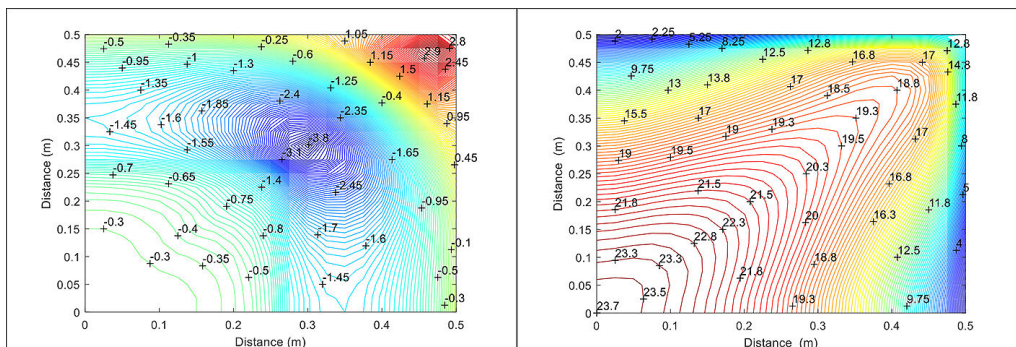


Figure 21. Maximum principal stress contours of SGP-connected undelaminated unit for 10 kPa pressure  
a) upper surface b) lower surface

Similar to the behavior of EVA connected unit, upper surface stresses are positive and negative and lower surface stresses are positive for the units connected by SGP as shown in Figures 20 and 21. For both delaminated and undelaminated units, the maximum principal compressive stress on the upper surfaces is located on the diagonal line. On the other hand, the lower surface's maximum principal stress occurs at the center for undelaminated unit and near the diagonal for the delaminated unit. Figures make it clear that the stress distribution in units that have delamination and those that don't is precisely different.

## CONCLUSIONS

Because of its unique qualities, including its longevity, high compressive strength, translucency, comparatively high tensile strength, and resilience to environmental influences, glass has become a more prominent structural material among architects in recent years. Despite the mentioned advantages of it, the fragile structure of glass is a significant problem. At this point, laminated glass emerges as a solution to various design problems. Since glass cannot flow plastically to relieve severe stresses, by inserting interlayers between the glass panes the stress capacity of laminated glass is increased and structural glass design is created.

This research study describes the investigations conducted on the delamination properties of laminated glass with different interlayers. Effect of delamination and structural performance of laminated glass are evaluated according to the properties of different interlayers. Nowadays, PVB is used most commonly and SGP is used less frequently. Several researches have been conducted to analyze the effect of alternative interlayers. Further investigation is needed to gain a clearer understanding of how these alternative interlayer materials react to delamination.

The strength and deflection behavior of laminated glass panes with initial delamination are obtained using the minimum potential energy theorem and variational method. Delaminated and undelaminated unit areas yield two distinct sets of equations with five coupled nonlinear differential equations. The finite difference method is used to derive the discrete form of differential equations. Matrix equations are solved using specific solvers. Difficulties with convergence are overcome by utilizing a variable under relaxation

factor for  $w$  and progressively increasing the load for a convergent solution. Analysis of laminated glass with different interlayer properties, support conditions and loadings are generated with the developed model.

Interlayer properties have proved to be an important factor in the structural performance of laminated and delaminated glass. The selection of interlayer type can cause significant variations in the strength of laminated glass with delamination. This study examines effects of three types of interlayer case; Polyvinyl Butyral (PVB), Ethyl Vinyl Acetate (EVA) and SentryGlas® Plus (SGP). Laminated and delaminated glass plate deflection and strength were observed as dependent on the interlayer type. The mechanical characteristics of laminated glass have been extensively examined, with a focus on PVB and SGP linked units. Given the significance of delamination, further study into alternative interlayers is needed.

The author draws the conclusion that PVB, the most widely used interlayer material, isn't always the best choice for all applications based on the information gathered. PVB exhibits good adherence to glass as well as transparency during the lamination process. SGP, on the other hand, is tougher and stiffer than standard PVB, it adheres well to glass and demonstrates significant structural performance advantages over EVA and PVB. The different behaviors of PVB, EVA and SGP-connected laminated glass with and without delamination can be attributed to their differences in shear modulus. Differences in shear modulus have a significant impact on delamination behavior due to the definition of this phenomenon. As the shear modulus increases, the effect of delamination becomes more noticeable. Undelaminated glass plates experience higher stress levels, including compression and tension, compared to delaminated units.

The results of this study have shown that where delamination is a major concern, interlayer type was the predominant effective structural factor. Additionally, boundary conditions have an impact on how a delaminated glass plate behaves. When comparing deflection and stress values for delaminated versus undelaminated units, the effect of delamination is more pronounced in simply supported plates than in those with fixed supports. Although SGP interlayer provides laminated glass with superior performance in terms of strength, safety, durability, sound insulation, UV protection, and overall visual appeal the effect

of delamination is more observable in laminated glass units connected by SGP. While the effect of delamination is more observable for SGP connected units among the three, followed by EVA, and then PVB.

## REFERENCES

- Hooper J.A., On the bending of architectural laminated glass. *Int. J. Mech. Sci.* 1973; 15: 309–323. [https://doi.org/10.1016/0020-7403\(73\)90012-X](https://doi.org/10.1016/0020-7403(73)90012-X).
- Behr R.A., Minor J.E., Linden M.P., Vallabhan C.V.G., Laminated glass units under uniform lateral pressure. *ASCE J. Struct. Eng.* 1984; 111(5): 1037–1050. [https://doi.org/10.1061/\(ASCE\)0733-9445\(1985\)111:5\(1037\)](https://doi.org/10.1061/(ASCE)0733-9445(1985)111:5(1037)).
- Minor J.E., Developments in the design of architectural glazing systems. *First Natl Struct. Eng. Conf., Australia*, 1987; 77.
- Behr R.A., Minor J.E., Linden M.P., Load duration and interlayer thickness effects on laminated glass. *J. Struct. Eng.* 1986; 112(6): 1441–1453. [https://doi.org/10.1061/\(ASCE\)0733-9445\(1986\)112:6\(1441\)](https://doi.org/10.1061/(ASCE)0733-9445(1986)112:6(1441)).
- Vallabhan C.V.G., Minor J.E., Nagalla S.R., Stresses in layered glass units and monolithic glass plates. *J. Struct. Eng.* 1987; 113: 36–43. [https://doi.org/10.1061/\(ASCE\)0733-9445\(1987\)113:1\(36\)](https://doi.org/10.1061/(ASCE)0733-9445(1987)113:1(36)).
- Vallabhan C.V.G., Das Y.C., Magdi M., Asik M.Z., Bailey J.R., Analysis of laminated glass units. *J. Struct. Eng.* 1993; 119: 1572–1585. [https://doi.org/10.1061/\(ASCE\)0733-9445\(1993\)119:5\(1572\)](https://doi.org/10.1061/(ASCE)0733-9445(1993)119:5(1572)).
- Behr R.A., Minor J.E., Norville S.H., Structural behavior of architectural laminated glass. *J. Struct. Eng.* 1993; 119: 202–222. [https://doi.org/10.1061/\(ASCE\)0733-9445\(1993\)119:1\(202\)](https://doi.org/10.1061/(ASCE)0733-9445(1993)119:1(202)).
- Minor J.E., Reznik P.L., Failure strengths of laminated glass. *J. Struct. Eng.* 1990; 116(4): 1030–1039. [https://doi.org/10.1061/\(ASCE\)0733-9445\(1990\)116:4\(1030\)](https://doi.org/10.1061/(ASCE)0733-9445(1990)116:4(1030)).
- Asik M.Z., Tezcan S., A mathematical model for the behavior of laminated glass beams. *Comput. Struct.* 2005; 83 (21–22): 1742–1753. <https://doi.org/10.1016/j.compstruc.2005.02.020>.
- Naumenko K., Eremeyev V.A., A layer-wise theory for laminated glass and photovoltaic panels. *Compos. Struct.* 2014; 112:283–291. <https://doi.org/10.1016/j.compstruct.2014.02.009>.
- Eisenträger J., Naumenko K., Altenbach H., Meenen J., A user-defined finite element for laminated glass panels and photovoltaic modules based on a layer-wise theory. *Compos. Struct.* 2015;133:265–277. <https://doi.org/10.1016/j.compstruct.2015.07.049>.
- Focacci F., Foraboschi P., De Stefano M., Composite beam generally connected: analytical model. *Compos. Struct.* 2015; 133: 1237–1248. <https://doi.org/10.1016/j.compstruct.2015.07.044>.
- Overend M., Butchart C., Lambert H., Prassas M., The mechanical performance of laminated hybrid-glass units. *Compos. Struct.* 2014; 110: 163–173. <https://doi.org/10.1016/j.compstruct.2013.11.009>.
- Ma Q., Wu L., Huang D., An extended peridynamic model for dynamic fracture of laminated glass considering interfacial debonding. *Compos. Struct.* 2022; 290: 115552. <https://doi.org/10.1016/j.compstruct.2022.115552>.
- Chen S., Zang M., Xua W., A three-dimensional computational framework for impact fracture analysis of automotive laminated glass. *Comput. Methods Appl. Mech. Eng.* 2015; 294: 72–99. <https://doi.org/10.1016/j.cma.2015.06.005>.
- Xu X., Chen S., Wang D., Zang M., An efficient solid-shell cohesive zone model for impact fracture analysis of laminated glass. *Theor. Appl. Fract. Mech.* 2020; 108: 102660. <https://doi.org/10.1016/j.tafmec.2020.102660>.
- Gao W., Xin L., Chen S., Bui T.Q., Yoshimura S., A cohesive zone based DE/FE coupling approach for interfacial debonding analysis of laminated glass. *Theor. Appl. Fract. Mech.* 2020; 108: 102668. <https://doi.org/10.1016/j.tafmec.2020.102668>.
- Gao W., Wanga R., Chen S., Yin S., Zang M., An intrinsic cohesive zone approach for impact failure of windshield laminated glass subjected to a pedestrian headform. *Int. J. Impact Eng.* 2019; 129: 147–159. <https://doi.org/10.1016/j.ijimpeng.2018.12.013>.
- Chen S., Zang M., Wang D., Yoshimura S., Yamada T., Numerical analysis of impact failure of automotive laminated glass: a review. *Compos. B Eng.* 2017; 122: 47–60. <https://doi.org/10.1016/j.compositesb.2017.04.007>.
- Timmel M., Kolling S., Osterrieder P., Du Bois P.A., A finite element model for impact simulation with laminated glass. *Int. J. Impact Eng.* 2007; 34(8): 1465–1478, <https://doi.org/10.1016/j.ijimpeng.2006.07.008>.
- Chen S., Zang M., Xu W., A three-dimensional computational framework for impact fracture analysis of automotive laminated glass. *Comput. Methods Appl. Mech. Eng.* 2015; 294: 72–99. <https://doi.org/10.1016/j.cma.2015.06.005>.
- Wang X., Yang J., Liu Q., Zhao C., Experimental investigations into SGP laminated glass under low velocity impact. *Int. J. Impact Eng.* 2018; 122: 91–108, <https://doi.org/10.1016/j.ijimpeng.2018.06.010>.
- Lenci S., Consolini L., Clementi F., On the experimental determination of dynamical properties of laminated glass. *Ann. Solid Struct. Mech.* 2015; 7: 27–43. <https://doi.org/10.1007/S12356-015-040-z>.
- Kozłowski M., Experimental and numerical

- assessment of structural behaviour of glass balustrade subjected to soft body impact. *Compos. Struct.* 2019; 229: 111380. <https://doi.org/10.1016/j.compstruct.2019.111380>.
25. J. Franz, Investigation of the residual load-bearing behaviour of fractured glazing. TU Darmstadt; 2015,
26. Bedon C., Issues on the vibration analysis of in-service laminated glass structures: analytical, experimental and numerical investigations on delaminated beams. *Appl. Sci.* 2019; 9 (18): 3928. <https://doi.org/10.3390/app9183928>
27. Chen X., Chan A.H.C., Modelling impact fracture and fragmentation of laminated glass using the combined finite-discrete element method. *Int. J. Impact Eng.* 2018; 112: 15–29. <https://doi.org/10.1016/j.ijimpeng.2017.10.007>
28. Lei Z., Rougier E., Knight E.E., Zang M., Munjiza A., Impact fracture and fragmentation of glass via the 3D combined finite-discrete element method. *Appl. Sci.* 2021; 11 (6): 2484. <https://doi.org/10.3390/app11062484>
29. Bermbach T., Teich M., Gebbeken N., Experimental investigation of energy dissipation mechanisms in laminated safety glass for combined blast-temperature loading scenarios. *Glass Struct. Eng.* 2016; 1 (1): 331–350. DOI 10.1007/s40940-016-0029-y
30. Pelfrene J., Kuntsche J., Van Dam S., Van Paepegem W., Schneider J., Critical assessment of the post-breakage performance of blast loaded laminated glazing: experiments and simulations. *Int. J. Impact Eng.* 2016; 88: 61–71. <https://doi.org/10.1016/j.ijimpeng.2015.09.008>
31. Dural E., Oyar F., Effect of delamination size, location and boundary conditions on the behavior of a laminated glass plate. *Struct.* 2023; 47: 121–133. <https://doi.org/10.1016/j.istruc.2022.11.034>
32. Asik M.Z., Laminated glass plate: Revealing of non-linear behavior. *Comput. Struct.* 2003; 81: 2659–71. [https://doi.org/10.1016/S0045-7949\(03\)00325-0](https://doi.org/10.1016/S0045-7949(03)00325-0).
33. Del Linz P., Hooper P.A., Arora H., Wang Y., Smith D., Blackman B.R., et al., Delamination properties of laminated glass windows subject to blast loading. *Int. J. Impact Eng.* 2017; 105: 39–53. <https://doi.org/10.1016/j.ijimpeng.2016.05.015>.
34. Dural E., Analysis of delaminated glass beams subjected to different boundary conditions. *Compos. B.* 2016; 101: 132–146. <https://doi.org/10.1016/j.compositesb.2016.07.002>.
35. Vedrtnam A., Experimental and simulation studies on delamination strength of laminated glass composites having polyvinyl butyral and ethyl vinyl acetate inter-layers of different critical thicknesses. *Def. Technol.* 2018; 14: 313–317. <https://doi.org/10.1016/j.dt.2018.02.002>.
36. Chen X., Rosendahl P.L., Chen S., Schneider J., On the delamination of polyvinyl butyral laminated glass: identification of fracture properties from numerical modelling. *Construct. Build. Mater.* 2021; 306: 124827. <https://doi.org/10.1016/j.conbuildmat.2021.124827>.
37. Davies P., Cadwallader R., Delamination Issues with Laminated Glass – Causes and Prevention; Glass Processing Days Finland, 2003.
38. Ja’skowiec J., Numerical modeling mechanical delamination in laminated glass by XFEM. *Procedia Eng.* 2015; 108: 293–300. <https://doi.org/10.1016/j.proeng.2015.06.150>.
39. Bedon C., Issues on the vibration analysis of in-service laminated glass structures: analytical, experimental and numerical investigations on delaminated beams. *Appl. Sci.* 2019; 9 (18): 3928. <https://doi.org/10.3390/app9183928>.
40. Chen S., Chen Z., Chen X., Schneider J., Evaluation of the delamination performance of polyvinyl-butyl laminated glass by through-cracked tensile tests. *Construct. Build. Mater.* 2022; 341: 127914. <https://doi.org/10.1016/j.conbuildmat.2022.127914>.
41. Campione G., Orlando F., Fileccia X., Pauletta M., Bond characterization of monolithic and layered glass panels and ultrasonic tests to control glued surfaces. *Eng. Struct.* 2019; 198: 109545. <https://doi.org/10.1016/j.engstruct.2019.109545>.
42. Wang X., Yang J., Wang F., Liu Q., Xu H., Simulating the impact damage of laminated glass considering mixed mode delamination using FEM/DEM. *Compos. Struct.* 2018; 202: 1239–1252. <https://doi.org/10.1016/j.compstruct.2018.05.127>.
43. Poblete F.R., Mondal K., Ma Y., Dickey M.D., Genzer J., Zhu Y., Direct measurement of rate-dependent mode I and mode II traction-separation laws for cohesive zone modeling of laminated glass. *Compos. Struct.* 2022; 279: 114759. <https://doi.org/10.1016/j.compstruct.2021.114759>.
44. Shahriari M., Googarchi H.S., Prediction of vehicle impact speed based on the post-cracking behavior of automotive PVB laminated glass: analytical modeling and numerical cohesive zone modeling. *Eng. Fract. Mech.* 2020; 240:107352. <https://doi.org/10.1016/j.engfracmech.2020.107352>.
45. Gao W., Liu X., Chen S., Bui T.Q., Yoshimura S. A cohesive zone based DE/FE coupling approach for interfacial debonding analysis of laminated glass. *Theor. Appl. Fract. Mech.* 2020; 108: 102668. <https://doi.org/10.1016/j.tafmec.2020.102668>.
46. Turon A., D’ avila C.G., Camanho P.P., Costa J., An engineering solution for mesh size effects in the simulation of delamination using cohesive zone models. *Eng Fract Mech.* 2007; 74 (10): 1665–1682. <https://doi.org/10.1016/j.engfracmech.2006.08.025>.
47. Rahul-Kumar P., Jagota A., Bennison S.J., Saigal S., Interfacial failures in a compressive shear strength test of glass/polymer laminates. *Int. J. Solid Struct.*

- 2000; 37: 7281–7305. [https://doi.org/10.1016/S0020-7683\(00\)00199-2](https://doi.org/10.1016/S0020-7683(00)00199-2).
48. Muralidhar S., Jagota A., Bennison S.J., Saigal S., Mechanical behaviour in tension of cracked glass bridged by an elastomeric ligament. *Acta Mater.* 2000; 48: 4577–4588. [https://doi.org/10.1016/S1359-6454\(00\)00244-5](https://doi.org/10.1016/S1359-6454(00)00244-5).
49. Butchart C., Overend M., Delamination in fractured laminated glass, in: *Engineered Transparency; International Conference at Glasstec, Dusseldorf, Germany, 2012.*
50. Iwasaki R., Sato C., Latailladeand J.L., Viot P., Experimental study on the interface fracture toughness of PVB (polyvinyl butyral)/glass at high strain rates. *Int. J. Crashworthiness.* 2007; 12: 293–298. <https://doi.org/10.1080/13588260701442249>.
51. Dural E., Vural S., Influence of boundary conditions on the behavior of laminated glass curved beam with delamination effect: An experimental and numerical investigation. *Heliyon.* 2024; 10: e24253. <https://doi.org/10.1016/j.heliyon.2024.e24253>
52. Dural E. Experimental and numerical treatment of delamination in laminated glass plate structures. *J J Reinf Plast Comp* 2016;35(1):56–70. <https://doi.org/10.1016/j.compositesb.2013.11.004>.
53. Bagaskara A., Rachmawati , Suwarno, Environmental Effects on Parameters of Leakage Current Equivalent Circuits of Outdoor Insulators. *Emerg. Sci. J.* 2024; 8(1): 310-325. <http://dx.doi.org/10.28991/ESJ-2024-08-01-022>
54. Maraqa F., Yasin A.A. 1 ,Al-Sahawneh E., Alomari J , Al-Adwan J , Al-Elwan A. A., Artificial Neural Network-Based Prediction of Physical and Mechanical Properties of Concrete Containing Glass Aggregates. *Civ. Eng. J.* 2024;10(5): 1627-1644. <http://dx.doi.org/10.28991/CEJ-2024-010-05-018>
55. Al Khazaleh M., Kumar P.K., Qtiasha D., Alqatawna A., Experimental Study on Strength and Performance of Foamed Concrete with Glass Powder and Zeolite. *Civ. Eng. J.* 2024; 10(12): 3911-3925. <http://dx.doi.org/10.28991/CEJ-2024-010-12-06>